The Journal of Experimental Biology 216, 1280-1291

doi:10.1242/jeb.074773

## RESEARCH ARTICLE

# Feed-forward and visual feedback control of head roll orientation in wasps (*Polistes humilis*, Vespidae, Hymenoptera)

Stéphane Viollet[1,*] and Jochen Zeil[2]

[1]Aix-Marseille Université, CNRS, ISM UMR 7287, CP 910, 13288, Marseille Cedex 09, France and [2]ARC Centre of Excellence in Vision Science, Research School of Biology, The Australian National University, Biology Place, Building 46, Canberra, ACT 0200, Australia

*Author for correspondence (stephane.viollet@univ-amu.fr)

### SUMMARY

**Flying insects keep their visual system horizontally aligned, suggesting that gaze stabilization is a crucial first step in flight control. Unlike flies, hymenopteran insects such as bees and wasps do not have halteres that provide fast, feed-forward angular rate information to stabilize head orientation in the presence of body rotations. We tested whether hymenopteran insects use inertial (mechanosensory) information to control head orientation from other sources, such as the wings, by applying periodic roll perturbations to male *Polistes humilis* wasps flying in tether under different visual conditions indoors and in natural outdoor conditions. We oscillated the thorax of the insects with frequency-modulated sinusoids (chirps) with frequencies increasing from 0.2 to 2 Hz at a maximal amplitude of 50 deg peak-to-peak and maximal angular velocity of ±245 deg $s^{-1}$. We found that head roll stabilization is best outdoors, but completely absent in uniform visual conditions and in darkness. Step responses confirm that compensatory head roll movements are purely visually driven. Modelling step responses indicates that head roll stabilization is achieved by merging information on head angular velocity, presumably provided by motion-sensitive neurons and information on head orientation, presumably provided by light level integration across the compound eyes and/or ocelli (dorsal light response). Body roll in free flight reaches amplitudes of ±40 deg and angular velocities greater than 1000 deg $s^{-1}$, while head orientation remains horizontal for most of the time to within ±10 deg. In free flight, we did not find a delay between spontaneous body roll and compensatory head movements, and suggest that this is evidence for the contribution of a feed-forward control to head stabilization.**

Supplementary material available online at http://jeb.biologists.org/cgi/content/full/216/7/1280/DC1

Key words: *Polistes* wasps, head roll control, vision, efference copy, feed-forward control, modelling, visuo-motor feedback loop, gaze control.

Received 11 May 2012; Accepted 6 December 2012

## INTRODUCTION

Hymenopteran insects such as honeybees and solitary wasps stabilize their head around roll and pitch axes during flight (Zeil et al., 2008; Boeddeker and Hemmi, 2010; Boeddeker et al., 2010). Such compensatory head movements have been thoroughly studied in flies, where a significant contribution to head stabilization comes from non-visual, mechanosensory input from modified wings, called halteres (Hengstenberg, 1993; Nalbach, 1993; Nalbach, 1994; Nalbach and Hengstenberg, 1994; Dickinson, 1999; Sherman and Dickinson, 2003; Fox and Daniel, 2008; Huston and Krapp, 2009; Frye, 2009). Here we ask whether compensatory head movements in hymenopteran insects, which lack the fast, feed-forward, mechanosensory input from Coriolis force-sensing modified wings, are driven not only by visual input (Boeddeker and Hemmi, 2010) but also by mechanosensory input that may be originating from mechanoreceptors on the wings, as suggested by Pix et al. (Pix et al., 1993) or at the base of the antennae, as has been demonstrated in moths (Sane et al., 2007).

We used male *Polistes* wasps in this study, rather than honeybees, because they readily fly when tethered and also continue to do so in the dark. We oscillated the tethered wasps around the roll axis in different visual conditions: within an opaque, horizontal cylinder in complete darkness; with a homogeneously illuminated, featureless white wall; with a horizontal pattern of regular black and white stripes; and with an artificial horizon, in full view of a cluttered and well-lit indoor environment and of a natural visual environment outdoors. We found no evidence for mechanosensory input to the system that stabilizes the head around the roll axis in these wasps. To explain visual control of head roll, we provide a control scheme for purely visually mediated head stabilization based on two nested visual feedback loops involving the measurement of head angular rate and its orientation. We also analysed head roll control in free flight, and suggest that its delay-less compensation for body roll is evidence for an efference copy of the body control input signal in spontaneous roll manoeuvres.

## MATERIALS AND METHODS

### General procedure

Male wasps (*Polistes humilis* Fabricius) were captured at their nest, kept in foam-stopper vials and provided with sugar solution on cotton tips. Before preparing a wasp for an experiment we always checked whether the wasp could fly by releasing and recapturing it indoors. Wasps were held in a foam clamp and a small piece of cardboard was waxed to the thorax. The wasps were then fixed coaxially to the shaft of a servomotor via a flexible wire and a tiny clip that held

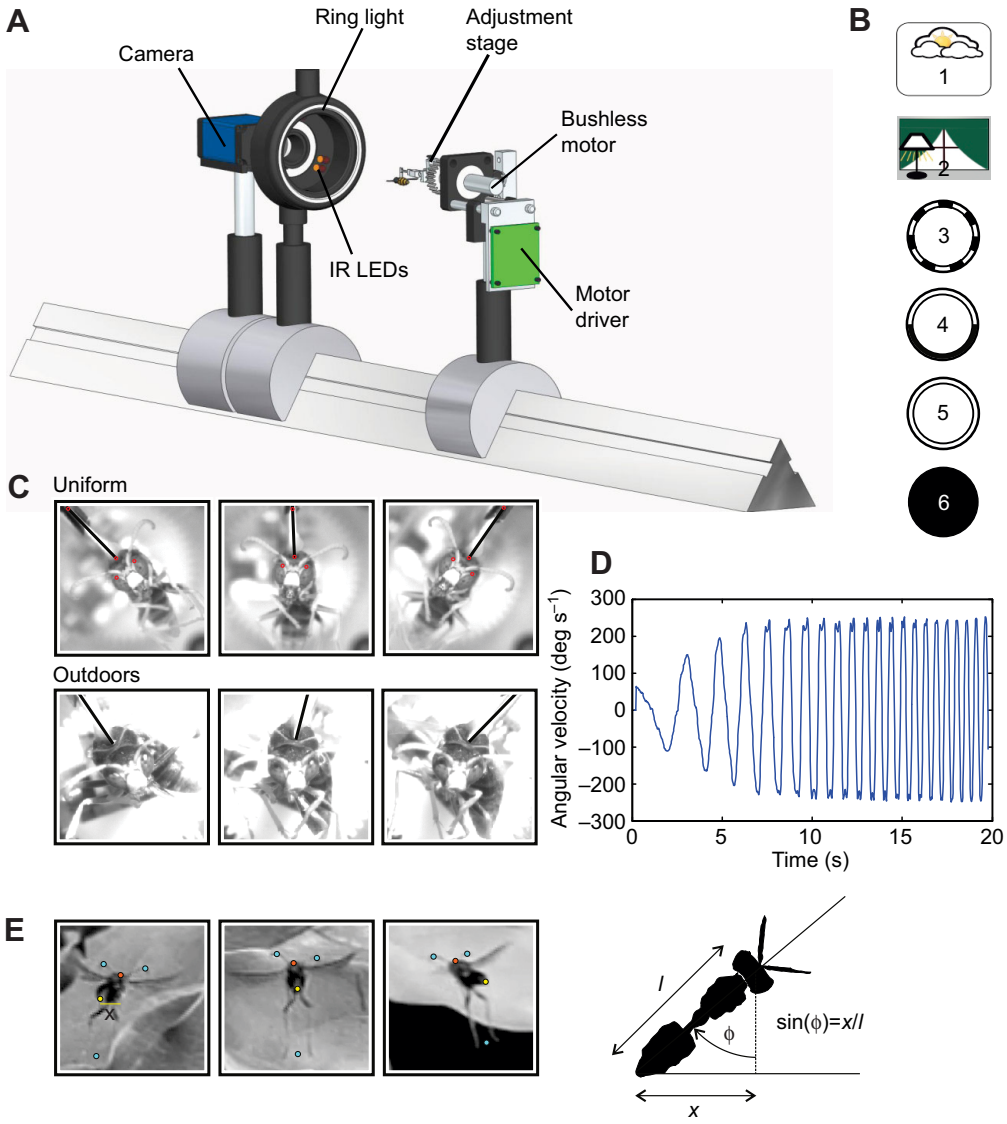


Fig. 1. Experimental set-up to determine compensatory head roll movements in *Polistes* wasps. (A) Wasps were tethered by waxing a strip of cardboard to their thorax and mounted onto the shaft of a servo motor, which was used to rotate the body of the wasp. Wasps viewed different visual scenes (B): a natural, outdoor environment (B1), a cluttered and artificially lit indoor laboratory environment (B2), a regular pattern of black and white stripes inside an opaque tube (B3), an artificial horizon (B4), a homogeneous white background (B5), or a completely dark environment (B6). Patterns inside an opaque horizontal cylindrical drum were illuminated with a fibre-optic ring-light and three pairs of infrared LEDs (in case of B6). Wasps were filmed head-on with a digital movie camera at 50 or 120 frames $s^{-1}$. (C) Sample images of head and body orientation in the two visual conditions outdoors and with a uniform white pattern. The points on the head and the holding structure that were used to determine orientation are marked by red dots. Note the lack of head roll compensation in the uniform condition. (D) The velocity profile of the chirp signal applied to the servo motor (see Materials and methods for details). (E) Three snapshots from movie records of male *Polistes* in free flight. The head and the tip of the abdomen are marked by red and yellow dots, respectively. Their horizontal distance ($x$), together with independent measurements of the length of the wasps' body long axis ($l$) was used to estimate the yaw axis orientation ($\phi$) of wasps (see schematic on the right). The points used to determine head orientation and body roll orientation are marked with blue dots.

the small piece of cardboard (Fig. 1). The data we present are all from wasps that flew in this tethered state.

### Experimental set-up

A servomotor (Faulhaber 0620C006, reduction gear ratio of 1024; Croglio, Switzerland) was mounted on an optical bench so that its centre shaft faced a digital camera (Firefly MV; PointGrey Research Inc., Richmond, Canada) (Fig. 1A). The motor and the camera were controlled via a data acquisition board (USB 6128; National Instruments, Austin, TX, USA) and a Firewire bus. The shaft of the servomotor, the insect head and the optical axis of the camera were carefully aligned by means of two perpendicular translation stages mounted on the motor shaft, by adjusting the height and orientation of the camera above the optical bench and by adjusting the flexible wire that held the insect. We ensured proper alignment by minimizing the translational movements of the head during rotations. The motor with the attached insect was then pushed inside an opaque cylinder (diameter 8.5 cm, length 10 cm) that was mounted on a fibre-optic ring-light (Schott Australia, Frenchs Forest, Australia) connected to a cold light source (KL 1500; Schott). In addition, the wasp was illuminated by three pairs of infrared LEDs (OPE5685, wavelength 850 nm), arranged coaxially around the camera lens to record head movements in darkness. A gentle air stream was generated by a small fan beside the camera pushing air past the camera lens towards the flying insect. The inside of the cylinder carried three different black and white patterns (Fig. 1B): equally spaced horizontal stripes of 1.25 cm width (spatial frequency of 0.03 cycles $deg^{-1}$); a 180 deg black, 180 deg white pattern forming an artificial horizon; and a white piece of paper. Our patterns extended 200 deg in both azimuth and elevation at the head of the wasps and thus covered 56% of the panoramic visual field, with ±40 deg in the frontal and caudal visual fields remaining not stimulated by the patterns inside the cylinder. Experiments inside the cylinder were performed in a completely dark room. In addition, we recorded compensatory head movements without the cylinder so that wasps viewed the well-lit indoor environment of the laboratory and by taking the whole set-up outdoors, where the wasps were exposed to sunny midday light intensities in a natural scene including trees and the artificial structures of a courtyard, surrounded by large buildings. We measured light levels in these different conditions with an ILT 1700 radiometer (International Light Technologies, Peabody, MA, USA) equipped with a Factor 1 Sensor W12826 to be: dark, $0.04\times10^{-9}$ W $cm^{-2}$; uniform, $1.95\times10^{-3}$ W $cm^{-2}$; horizon, $2.38\times10^{-3}$ W $cm^{-2}$; stripes, $2.13\times10^{-3}$ W $cm^{-2}$; room light, $2.85\times10^{-4}$ W $cm^{-2}$; outdoors,

$3.3\times10^{-2}$ W cm$^{-2}$. Light was measured with a horizontally oriented cosine sensor placed at the position of the insect facing into the drum, or outdoors at the location of the wasp head facing forwards.

### Recording sessions

We recorded head movements around the roll axis by placing a wasp about 10 cm in front of the camera (Fig. 1C). We measured the performance of head roll compensation by applying a sine wave oscillation with linearly increasing frequency from 0.2 to 2 Hz, called a chirp signal with maximal amplitude of 50 deg peak-to-peak and a maximal angular velocity of ±245 deg s$^{-1}$ (Fig. 1D). The amplitude of the oscillation decreased with increasing frequency (see Fig. 2) due to the dynamics of the brushless servomotor. We also employed a fast ramp signal with the same maximal angular velocity to check for the presence of position error signals monitoring the orientation of the head. Both chirp and ramp signals were applied to the servomotor that was rigidly coupled to the thorax of the wasp. Images were captured at 50 frames s$^{-1}$ for the chirp signal and at 120 frames s$^{-1}$ for the ramp signal, with a resolution of 640×480 pixels. The synchronization between servomotor and image acquisition was achieved with a custom-written LabVIEW-based program (National Instruments) running on a PC. In darkness, the image acquisition was synchronized with flashes produced by the infrared ring-light. Movie sequences were stored frame by frame as uncompressed 8-bit tiff images for off-line processing.

### Data analysis

The head orientation ($\theta_{head}$) and body orientation ($\theta_{body}$) of wasps were manually digitized with a custom-written MATLAB-based (MathWorks, Natick, MA, USA) program (Jan Hemmi and Robert Parker, The Australian National University) by recording frame by frame the *x*/*y* positions of two markers at the lateral-most part of the head and two markers on the piece of cardboard that was attached to the thorax of the wasp (see Fig. 1C). By definition, we have the following relationship between $\theta_{head}$ and $\theta_{body}$:

$$\theta_{body} + \theta_{headbody} = \theta_{head}\,, \quad (1)$$

where $\theta_{headbody}$ is the angular position of the head with respect to the body.

For perfect compensation of a rotational movement of the body (in our case around the roll axis), the angular orientation $\theta_{headbody}$ must be equal and opposite to $\theta_{body}$. For the ideal case of $\theta_{head}=0$, Eqn 1 becomes $\theta_{headbody}(t)=-\theta_{body}(t)$. This means that the transfer function $H(s)$ between $\theta_{body}$ and $\theta_{headbody}$ must be equal to −1 in the case of perfect compensation. To summarize, we have:

$$H(s) = \theta_{headbody}(s)/\theta_{body}(s) = -1\,, \quad (2)$$

where $s$ is the Laplace variable.

By definition, Eqn 2 means that in the case of perfect compensation, the module of $H(s)$, denoted $|H(j\omega)|=1$ (i.e. 0 dB) and the phase denoted $\mathrm{Arg}(H(j\omega))=-180$ deg, with $\omega$ the frequency in rad s$^{-1}$.

To determine the Bode diagram, we estimated the gain $|H(j\omega)|$ and phase $\mathrm{Arg}(H(j\omega)$ of the transfer function $H(s)$ as follows:

$$H(s) = \theta_{headbody}/\theta_{body}\,. \quad (3)$$

Therefore, from Eqn 3 the gain and phase of $H(s)$ were computed as follows:

$$|H(j\omega)|_{dB} = (|\theta_{head} - \theta_{body}|)/|\theta_{body}| = |\theta_{headbody}|/|\theta_{body}| \quad (4)$$

and

$$\mathrm{Arg}\,(H(j\omega)) = \mathrm{Arg}\,(\theta_{headbody}/\theta_{body})\,. \quad (5)$$

The frequency response of $H(s)$ was then estimated by applying spectral analysis on the time series of $\theta_{body}$, $\theta_{headbody}$ and $\theta_{head}$ [using

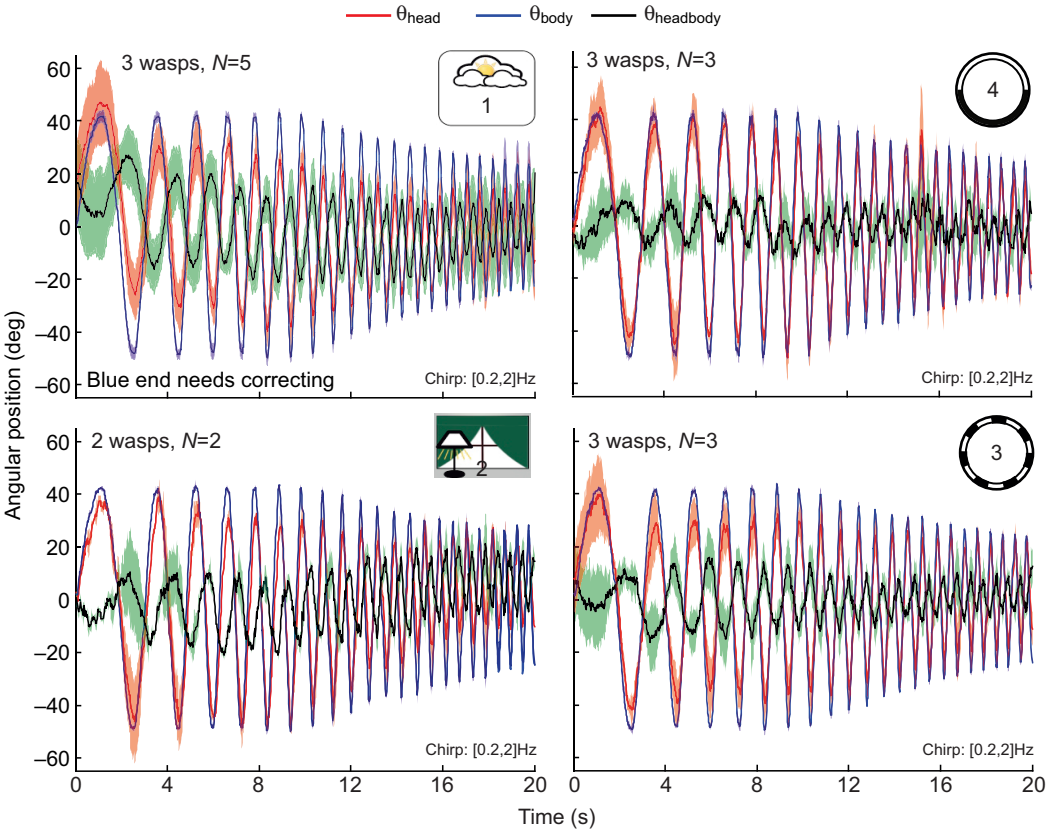


Fig. 2. Time course of head roll responses to sinusoidal, frequency modulated (chirp) oscillations applied to the body. In each of the four visual conditions indicated by pictograms (see Fig. 1B for explanation), the mean and s.d. (coloured envelope) of body orientation (blue), of head orientation (red) and of head orientation relative to the body (black and green) were plotted. The chirp signal frequency increased from 0.2 to 2 Hz in 20 s. Number of wasps and number of chirp runs averaged are given for each panel.

the MATLAB System Identification Toolbox 'spa' function, see Ljung (Ljung, 1999) for further details]. As discussed by Xia (Xia, 1997), the use of a chirp signal combined with a spectral analysis method allows one to use an efficient noise reduction technique based on the Fourier transform for the estimation of the transfer function of a linear system. Due to its better noise immunity, we therefore preferred spectral analysis over the classical method based on the Fourier transform (see Schwyn et al., 2011). The transfer function of a dynamical system can be directly estimated from the ratio of the Fourier transform of the output signal (here $\theta_{headbody}$) to the Fourier transform of the input signal (here $\theta_{body}$). For most of the time, irregularities and noise make this method (which has been called frequency analysis) difficult to use for the determination of the phase directly (see Ljung, 1996). We, therefore, preferred to use spectral analysis because it is less sensitive to noise. Spectral analysis allows one to estimate directly the transfer function from input and output signals by estimating the cross-spectrum between two signals (here $\theta_{body}$ and $\theta_{headbody}$) and the auto-spectrum of the input signal (here $\theta_{body}$) (see Ljung, 1996; Ljung, 1999). The cross-spectrum is defined by the Fourier transform of the cross-covariance function, whereas the auto-spectrum is the Fourier transform of the cross-spectrum with itself. The quality of the estimation depends on the Fourier transform method. A classical windowing method based on the Hamming window is the most common window used in spectral analysis. The choice of the window size is a pure trade-off between frequency resolution and the variance of the estimation.

The mean gain error is the mean of the error between the mean value of the gain $|H(j\omega)|$ of each wasp and 0 dB as follows: $\text{mean error}_{gain} = \text{mean}(0_{dB} - \text{mean}(|H(j\omega)|)$. The mean phase error is the mean of the error between the mean value of the phase $\text{Arg}(H(j\omega))$ of each wasp and –180 deg as follows: $\text{mean error}_{phase} = \text{mean}(180\,\text{deg} - \text{mean}(\text{Arg}(H(j\omega))))$.

When there was no compensation of the head orientation induced by roll movements of the thorax, it was not possible to compute the Bode diagram. In such cases we computed the cross-correlation between $\theta_{headbody}$ and $\theta_{body}$ and the autocorrelation function of $\theta_{body}$.

### Free flight recordings

Male *Polistes* wasps were filmed from behind with a horizontally levelled Casio Exilim EX-F1 camera at 300 frames $s^{-1}$ as they were regularly patrolling while often facing the branches of a *Magnolia* tree in Canberra, Australia in the autumn of 2012 (see supplementary material Movies 1–3). The camera was about 2 m away from the scene and viewed a recording area of 23.7×17.8 cm (6.8×5.1 deg) at an image size of 512×384 pixels. Perspective distortions were thus minimal. However, there are two remaining sources of errors in determining head and body roll orientations: errors in determining *x/y* coordinates from films (see below), and errors introduced by the fact that although the flight paths of the wasps were clearly perpendicular to the camera viewing direction, the orientation of the longitudinal body axis of the wasps was not always parallel to the optical axis of the camera. This introduces errors into the determination of body roll orientation, because it confuses body yaw movements with roll movements. In order to identify the parts of sequences in which the camera viewed animals from straight behind, we estimated their yaw orientation by the horizontal distance between the head and the tip of the abdomen (Fig. 1E), after having determined the average length of the longitudinal body axis of wasps to be 1.48±0.08 cm ($N$=16) from instances where wasps were clearly seen side-on (see supplementary material Fig. S1). For the correlation analysis, we only used those parts of sequences in which the yaw orientation of wasps was to within ±10 deg of the direction parallel to the camera optical axis. Note that this is a conservative criterion, because it also discards instances when the insects maintain large pitch angles during roll manoeuvres, which rotates the tip of the abdomen away from the midline.

We analysed 14 flight episodes, ranging from 0.34 to 1 s in length (8.14 s of total flight time), from which we extracted 13 sequences that fulfilled this criterion (3.75 s of total flight time), ranging from 0.17 to 0.43 s in length.

Sequences were stored as .mov-h264 encoded movies and sections showing flying wasps were exported as .jpeg sequences using QuickTimePro (Apple Inc., Cupertino, CA, USA). The *x/y* coordinates of the dorsal apex of antennae, the dorsal edge of the head and of the ventral-most point half-way between the long dangling hindlegs (blue and red dots in Fig. 1E) were extracted frame by frame using a MATLAB-based program, written by Jan Hemmi and Robert Parker (The Australian National University). Head orientation relative to the horizontal, and body orientation relative to the vertical (for easier comparison later rotated by 90 deg), were determined from the *x/y* coordinates using custom-written MATLAB programs. We estimated digitization errors by determining *x/y* coordinates for one sequence five times and calculating the mean and standard deviations for head and body orientation. The mean standard deviation was in all cases below 2 deg. The MATLAB xcorr function was used to calculate cross-correlations.

## RESULTS

We present our chirp data set in Fig. 2 for the four conditions that provided visual input (outdoors, indoors, striped pattern and horizon). Fig. 2 shows over time for each visual condition (see Fig. 1B) the mean value (thick lines) and standard deviation (s.d., coloured envelopes) of body orientation ($\theta_{body,}$ blue), head orientation ($\theta_{head}$, red) and the orientation of the head with respect to the body ($\theta_{headbody}$, black mean, green s.d.) for at least two wasps (see supplementary material Fig. S2 for all individual responses).

We note that head movements never compensate for more than about 50% of the imposed body roll movements at the relatively large oscillation amplitude we used, as is also the case in *Calliphora* (Hengstenberg, 1988). This was true for all conditions, in which pattern contrast was available (outdoors, indoors, stripe pattern and horizon). Perfect head roll compensation would mean that the head orientation of the wasp remains constant (i.e. $\theta_{head}$=0 deg) and $\theta_{headbody}$ and $\theta_{body}$ would change in anti-phase. Compensatory head movement amplitudes were always smaller than the amplitude of the imposed oscillation. In the frequency domain (Fig. 3), this under-compensation is reflected in a negative gain that was always smaller than 0 dB (gain<1) over the frequency range we tested (0.2–2 Hz). Perfect compensation would mean that the gain between $\theta_{headbody}$ and $\theta_{body}$ is equal to 1 (0 dB) and the phase is equal to –180 deg in the Bode plots (as indicated by the black dotted line in Fig. 3B,C). Table 1 shows the mean error between the real head roll compensation of wasps and the perfect case for each experimental condition.

The responses obtained in natural outdoor illumination conditions (Figs 2, 3) exhibit smaller gain and phase errors than those obtained for stripe and horizon patterns. Compensation is best in outdoor conditions with a mean gain error of 2 dB and a phase error of 9 deg ($N$=3 wasps, $n$=5 trials; Table 1). Outdoors, the gain remains nearly constant over the frequency range (blue line in Fig. 3B), but the mean phase value improves in the frequency range from 1 to 2 Hz, as the frequency of the oscillation increases and the amplitude decreases. We obtained similar results for the gain, but not the phase in the room light condition (red lines in Fig. 3B,C).

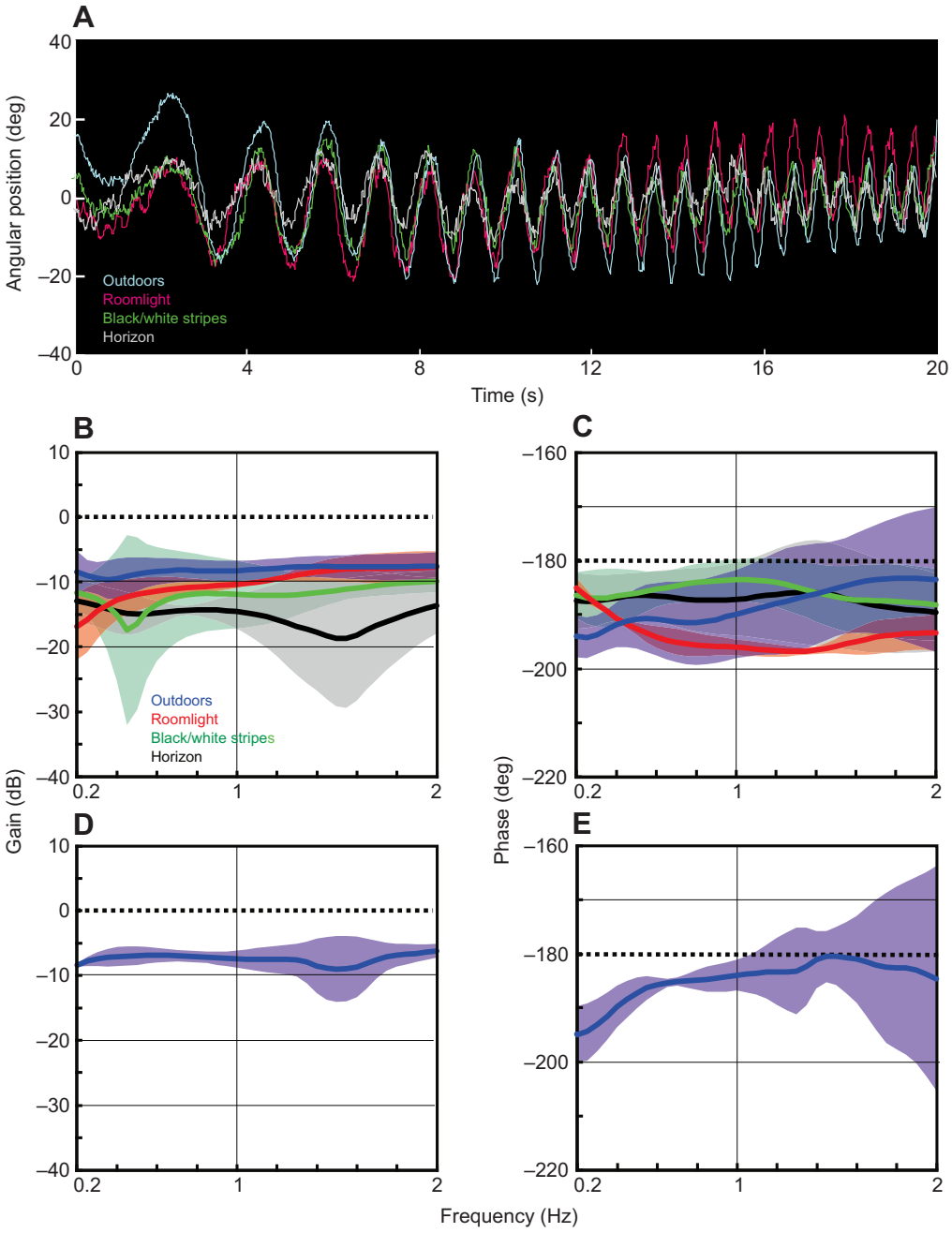


Fig. 3. Dynamic properties of the head roll response. (A) The mean chirp responses of the head in the four visual conditions: outdoors, room light, black/white stripes and horizon. (B) Bode diagram for the gain computed from the time course of responses shown in A. Thick lines are means and coloured areas are means ± s.d. Dotted line indicates perfect compensation of the head at 0 dB. (C) Bode diagram for the phase (perfect compensation at –180 deg indicated by dotted line); otherwise conventions as in B. Bode diagrams for the gain (D) and phase (E) for three stimulus repetitions outdoors obtained for one wasp.

The compensatory responses are similar in the striped pattern (green lines in Fig. 3B,C) and horizon conditions (black lines), although gain errors are on average larger than in the outdoor and indoor conditions (Table 1). In all the cases, the maximum mean phase is about –195 deg corresponding to a mean phase error of 15 deg (see Fig. 3C, Table 1), which means that the compensatory response has a mean time lag shorter or equal to two sampling periods (40 ms, see Fig. 4B). As far as average gain error is concerned, head compensation amplitude is smallest with the artificial horizon, which was the poorest visual stimulus in terms of spatial frequency composition.

To document intra-individual variability, Bode diagrams for three stimulus repetitions outdoors are shown for one wasp in Fig. 3D,E, together with means and standard deviation for an additional individual in the lower panel of Table 1.

When no pattern contrast was available in the uniform bright condition and in complete darkness, there was no evidence of any head roll compensation (Fig. 4A). The weak modulation of head orientation in the uniform condition was probably caused by some remaining visual structure within the apparatus and the small head movements in the dark condition were in the wrong direction. Head movement amplitudes were too small for the computation of the Bode diagrams. We therefore computed the autocorrelation function of body orientation $\theta_{body}$ and the cross-correlation function between $\theta_{body}$ and $-\theta_{headbody}$ (Fig. 4B). Compared with the four conditions that provided visual input, with maximal correlation coefficients between 0.7 and 0.9 and lags between 40 and 80 ms, the coefficients do not reach 0.4 in the uniform and –0.4 in the dark condition (Fig. 4B). We conclude that there are no detectable head movements that correlate with the sinusoidal oscillation of the wasp's body.

Table 1. Compensating errors

| | Gain error (dB) (*N*=32) | | Phase error (deg) (*N*=32) | |
|---|---|---|---|---|
| | Mean | s.d. | Mean | s.d. |
| Inter-individual variability | | | | |
| Outdoors (3 wasps, 5 trials) | 8.2 | 2.0 | 9.0 | 7.6 |
| Indoors (2 wasps, 2 trials) | 10.5 | 1.9 | 14.1 | 1.6 |
| Stripes (3 wasps, 3 trials) | 12.3 | 5.2 | 5.4 | 4.6 |
| Horizon (3 wasps, 3 trials) | 15.5 | 4.8 | 6.2 | 6.9 |
| Intra-individual variability (3 trials) | | | | |
| Wasp 1: outdoors | 7.6 | 2.0 | 4.9 | 4.8 |
| Wasp 2: outdoors | 9.2 | 1.6 | 15.3 | 6.2 |

The responses to imposed step changes in body orientation (Fig. 5) confirm that compensatory head movements are purely visually driven, but also provide two additional pieces of information. Outdoors, the wasps appear to have an absolute reference for head orientation because they were able to maintain a constant compensation angle of up to 20 deg when the body is turned 45 deg to the left or to the right (Fig. 5, left column). This cannot be due to a velocity servo, such as the optomotor response of the fly that stabilizes head yaw orientation by minimizing rotational optic flow around the yaw axis. Indeed, in a situation that does not provide angular position information, such as the regular black and white stripe pattern, wasps tend to be unable to keep head orientation constant after a step rotation (centre column, Fig. 5), indicating that the initial response of a velocity servo becomes corrected by a signal that adjusts head position relative to the thorax (Preuss and Hengstenberg, 1992; Gilbert and Bauer, 1998; Paulk and Gilbert, 2006). In full darkness (right column, Fig. 5), the head orientation of the wasp in some cases tends to overshoot the imposed rotation of the body and in some cases not. It is not clear at present why this should be so, but this observation again demonstrates that head orientation is not controlled by haltere-like mechanosensory input that would help to compensate for body rotations.

We attempted to model step responses of the head roll stabilization system in *Polistes* wasps by considering the angular orientation of the body as an input disturbance for two nested visual feedback loops: an outer position feedback loop based on the measurement of head orientation [transfer function $H_{eye}(s)$] and an inner speed feedback loop based on the measurement of the head rotational speed provided by wide-field motion sensitive neurons [transfer function $H_{MS}(s)$] with responses that could be similar to those of the VS neurons of the blowfly (Krapp et al., 1998). Fig. 6A shows on the left a block diagram of this model and on the right the different parameters of the transfer functions used to compute the model responses.

Model responses to 45 deg step changes of body orientation for $\theta_{head}(t)$ (grey lines in Fig. 6B) and for $\theta_{headbody}(t)$ (red lines in Fig. 6B) are very similar to the step responses we measured outdoors and in the presence of periodic stripes, with the exception of slight differences in steady-state values. Best fits for individual wasp

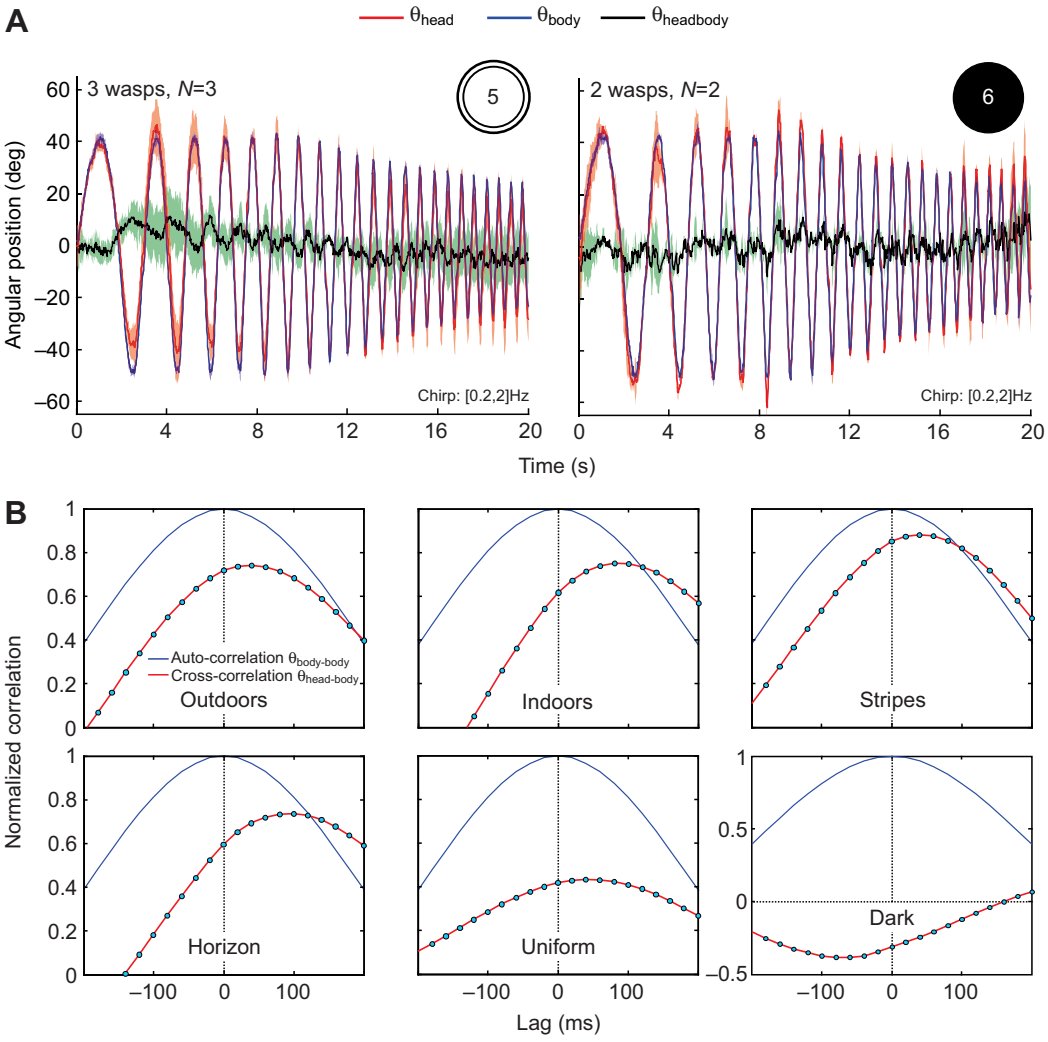


Fig. 4. Head roll responses in a uniform bright environment and in the dark. (A) Time course of head roll responses to sinusoidal, frequency-modulated (chirp) oscillations applied to the body. Conventions as in Fig. 2. (B) Autocorrelation of body oscillations (blue) and cross-correlation of body oscillation against the negative values of head movements relative to the body (red dotted line), for the ideal case: $\theta_{body}(t) = -\theta_{headbody}(t)$. The quality of compensation is indicated by a high correlation coefficient with some delay. Number of wasps and number of responses as in Fig. 2 for conditions horizon, stripes, indoor and outdoor. Uniform: responses obtained from three wasps (*N*=3) and three chirps in total (*n*=3). Dark: responses obtained from two wasps (*N*=2) and two chirps in total (*n*=2).

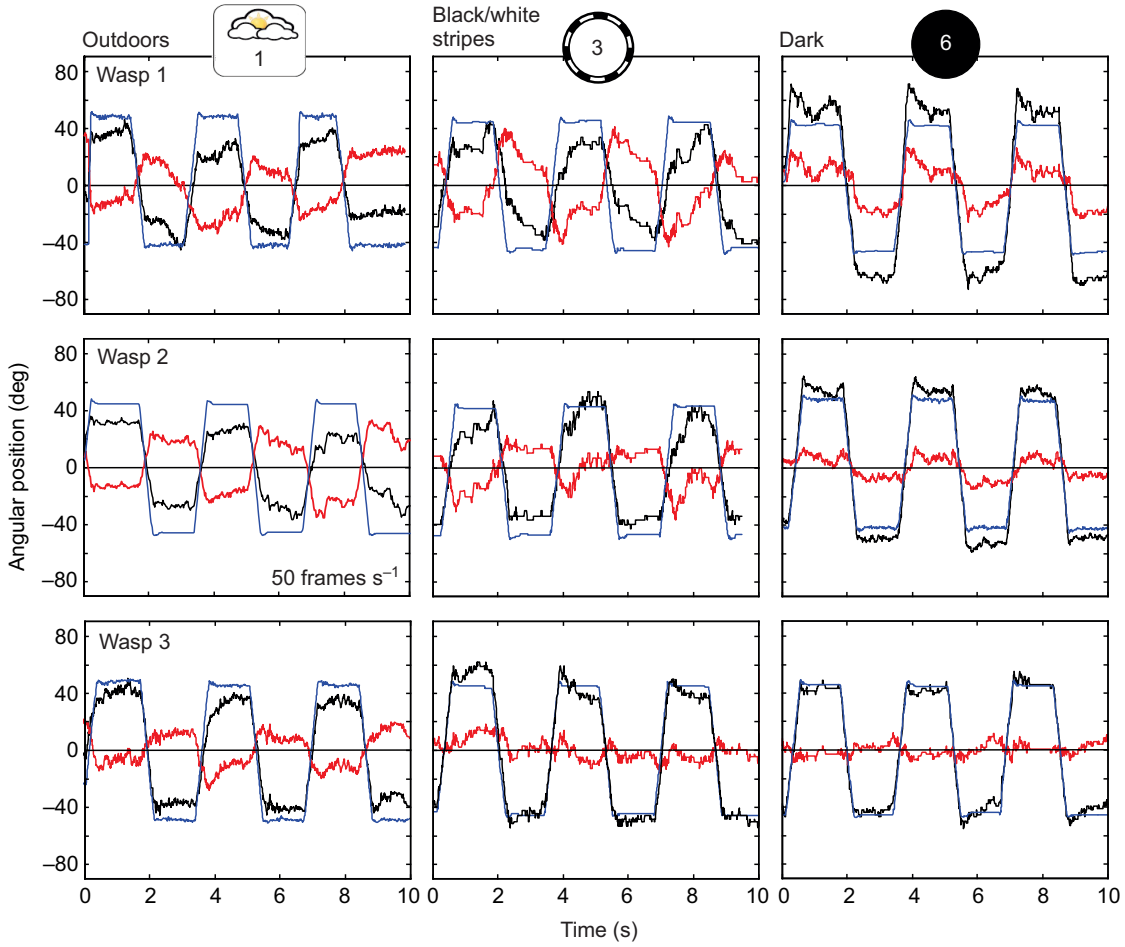


Fig. 5. Head roll responses of three wasps (top to bottom row) to step body rotations outdoors (left column), in a cylinder with black and white stripes (centre column) and in the dark (right column). Blue: body orientation; black: head orientation; red: head orientation relative to body.

responses required small adjustments in the values of the gain and the time constant of the transfer functions. The $H_{MS}(s)$ cut-off frequency indicates that outdoors, wasps should be able to respond to temporal frequencies of about 8 Hz, compared with 4 Hz in the indoor stripe environment.

In free flight, male *Polistes* wasps hold their heads horizontal to within ±10 deg despite body roll movements of more than ±40 deg. The four panels of Fig. 7A show the time course of head roll orientation ($\theta_{head}$ in red), of body roll orientation ($\theta_{body}$ in blue), of the inverse of head orientation relative to the body ($-\theta_{headbody}$ in black) and of the yaw orientation of the longitudinal body axis (in green). The sequence in the top panel of Fig. 7A was digitized five times to gain estimates of how accurately head and body orientation can be determined, with thick lines and equivalently shaded areas showing means ± s.d., respectively. Numbers on the right are the mean s.d. for the four variables. The grey horizontal bars in all panels of Fig. 7A mark the range of ±10 deg.

The distributions of head and body roll orientation during 3.75 s of flight (13 sequences, extracted from 14 flight episodes) during which wasps faced away from the camera to within ±10 deg confirm that the wasps keep their head aligned horizontally to within ±10 deg in the presence of body roll movements of up to 40 deg (Fig. 7B). Body roll oscillations in free flight thus do reach comparable amplitudes to the ones used in our experiments and the quality of head roll stabilization is as good as that reported for honeybees (Boeddeker and Hemmi, 2010). Naturally occurring angular velocities of the body tend to be predominantly below 500 deg $s^{-1}$ (Fig. 7B), so that the 245 deg $s^{-1}$ we used in our experiments were well within the natural range of velocities. Most surprisingly, in a cross-correlation analysis applied to 13 flight sequences, ranging from 0.17 to 0.43 s in length, we did not find detectable delays between body roll and head orientation (Fig. 7C, left panel), nor between the angular rates of body and head roll movements (Fig. 7C, right panel). Because our sampling interval was 3.33 ms at 300 frames $s^{-1}$, it seems unlikely that head stabilization is achieved by visual feedback, unless it is unusually fast in wasps. However, even the fast feed-forward signals from wing-based mechanoreceptors in flies require 3–5 ms to generate a head movement (Sandeman and Markl, 1980; Hengstenberg, 1993).

We did not find evidence for haltere-like mechanosensory input to the head stabilization system in response to imposed body roll rotations. The absence of a detectable and realistic delay in free flight thus suggests that the head may be stabilized by an efference copy signal. We modelled such a feed-forward control of the head orientation (Fig. 7D) as an extension of the two nested visual feedback loops (Fig. 6A) by considering a common drive signal $U_{roll}$ that elicits a spontaneous roll manoeuvre and controls both head and body orientation around the roll axis. A feed-forward controller $C_f(s)$ makes the head ($\theta_{headbody}$) compensate exactly for any rotation of the body ($\theta_{body}$).

According to the complete block diagram of the proposed head stabilization system (Fig. 7D), assuming that there is no

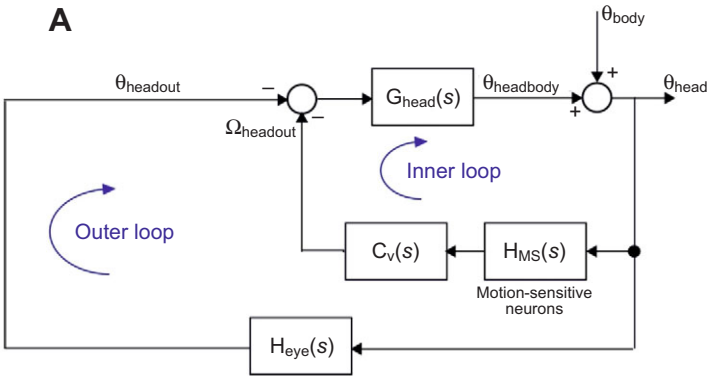


| | $H_{MS}(s)$ | $H_{eye}(s)$ | $C_v(s)$ | $G_{head}(s)$ |
|---|---|---|---|---|
| Wasp 1 outdoors | $\frac{0.05s}{(1+0.02s)}$ | $\frac{0.25}{(1+0.5s)}$ | $\frac{5}{(1+0.5s)}$ | $\frac{1}{(1+0.005s)}$ |
| Wasp 1 stripes | $\frac{0.1s}{(1+0.02s)}$ | 0 (openloop) | $\frac{5}{(1+0.5s)}$ | $\frac{1}{(1+0.005s)}$ |
| Wasp 2 outdoors | $\frac{0.05s}{(1+0.02s)}$ | $\frac{0.5}{(1+0.5s)}$ | $\frac{8}{(1+0.5s)}$ | $\frac{1}{(1+0.005s)}$ |
| Wasp 3 outdoors | $\frac{0.04s}{(1+0.02s)}$ | $\frac{0.27}{(1+0.5s)}$ | $\frac{5}{(1+0.5s)}$ | $\frac{1}{(1+0.005s)}$ |

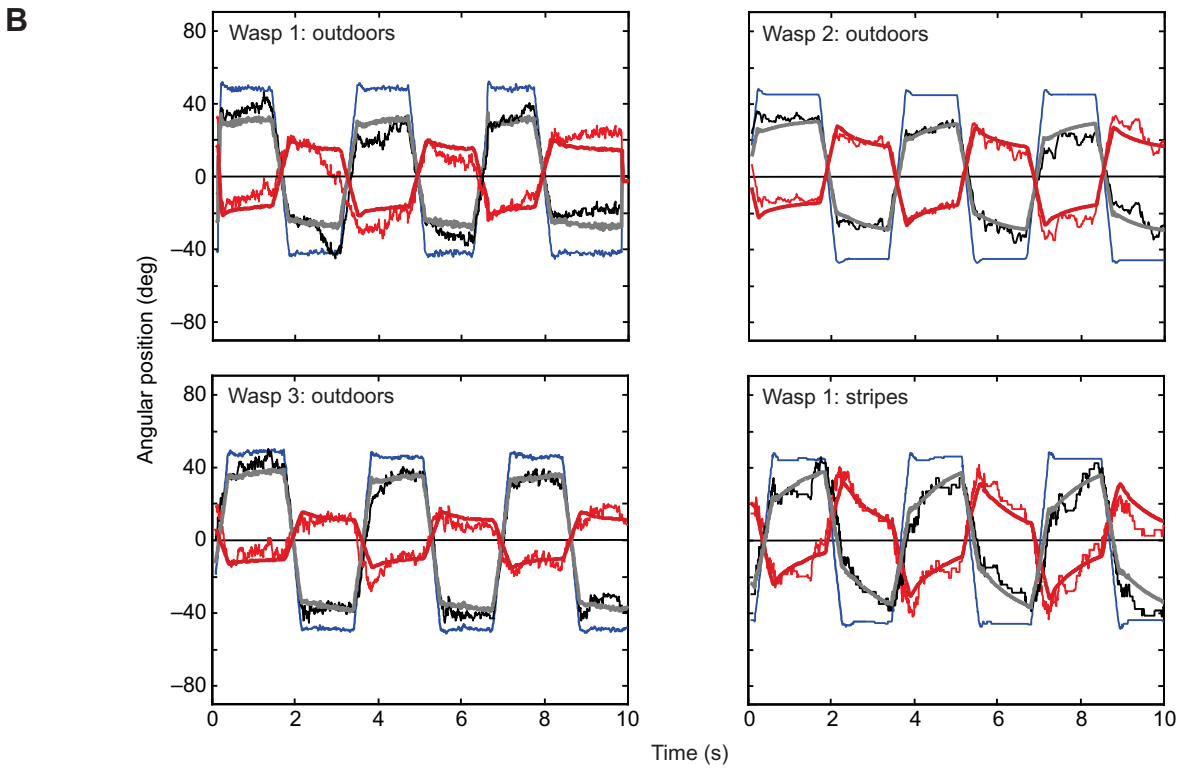


Fig. 6. Modelling head roll stabilization. (A) Left: block diagram of the head stabilization system in *Polistes* wasps based on two nested visual feedback loops. Right: transfer functions of the block diagram described on the left for model responses shown in B with $s$ as the Laplace variable. The inner feedback loop receives input on head angular speed ($\Omega_{headout}$) measured by motion-sensitive neurons [$H_{MS}(s)$] while the input to the outer feedback loop is the head orientation ($\theta_{headout}$) that could be measured by the tonic dorsal light response mediated by the compound eyes. The visual regulator $C_v(s)$ is a simple first-order low-pass filter removing the high-frequency components amplified by the derivative action of $H_{MS}(s)$. The head dynamics are modelled by a first-order low-pass filter with a time constant of 5 ms compatible with the low inertia and mass of the head. (B) Model performance compared with wasp step responses in outdoor and in black and white stripe conditions. Model responses $\theta_{head}(t)$ (thick grey lines) and $\theta_{headbody}(t)$ (thick red lines) were computed by taking measured body orientation $\theta_{body}(t)$ (blue lines) as input disturbance for the two nested visual feedback loops. Otherwise conventions as in Fig. 5.

disturbance applied to the body, the orientation of the head can be expressed as:

$$\theta_{head} = G_{body}(s)\, U_{roll} - G_{head}(s)\, C_f(s)\, U_{roll}\,. \quad (6)$$

For perfect compensation of a rotational movement of the body (in our case around the roll axis), the angular orientation $\theta_{headbody}$ must be equal and opposite to $\theta_{body}$, which means that $\theta_{head} = 0$. Then from Eqn 6, $C_f(s)$ can be written as:

$$C_f(s) = \hat{G}_{body}(s)/\hat{G}_{head}(s)\,, \quad (7)$$

with $\hat{G}_{body}(s)$ and $\hat{G}_{head}(s)$ the estimated transfer functions of $G_{body}(s)$ and $G_{head}(s)$, respectively. The thick grey and red lines in the three lower panels of Fig. 7A show the output of this model using the following transfer functions:

$$C_f(s) = 0.65/(1+2.10^{-3}\, s) \quad (8)$$

and

$$G_{head}(s) = 1/(1+1.10^{-3}\, s)\,, \quad (9)$$

while the other transfer functions remained the same as those used for wasp 1 outdoors (see Fig. 6A). Then from Eqn 7, $\hat{G}_{body}(s)$ and $\hat{G}_{head}(s)$ can be written as:

$$\hat{G}_{body}(s) = 1/(1+2.10^{-3}\, s) \quad (10)$$

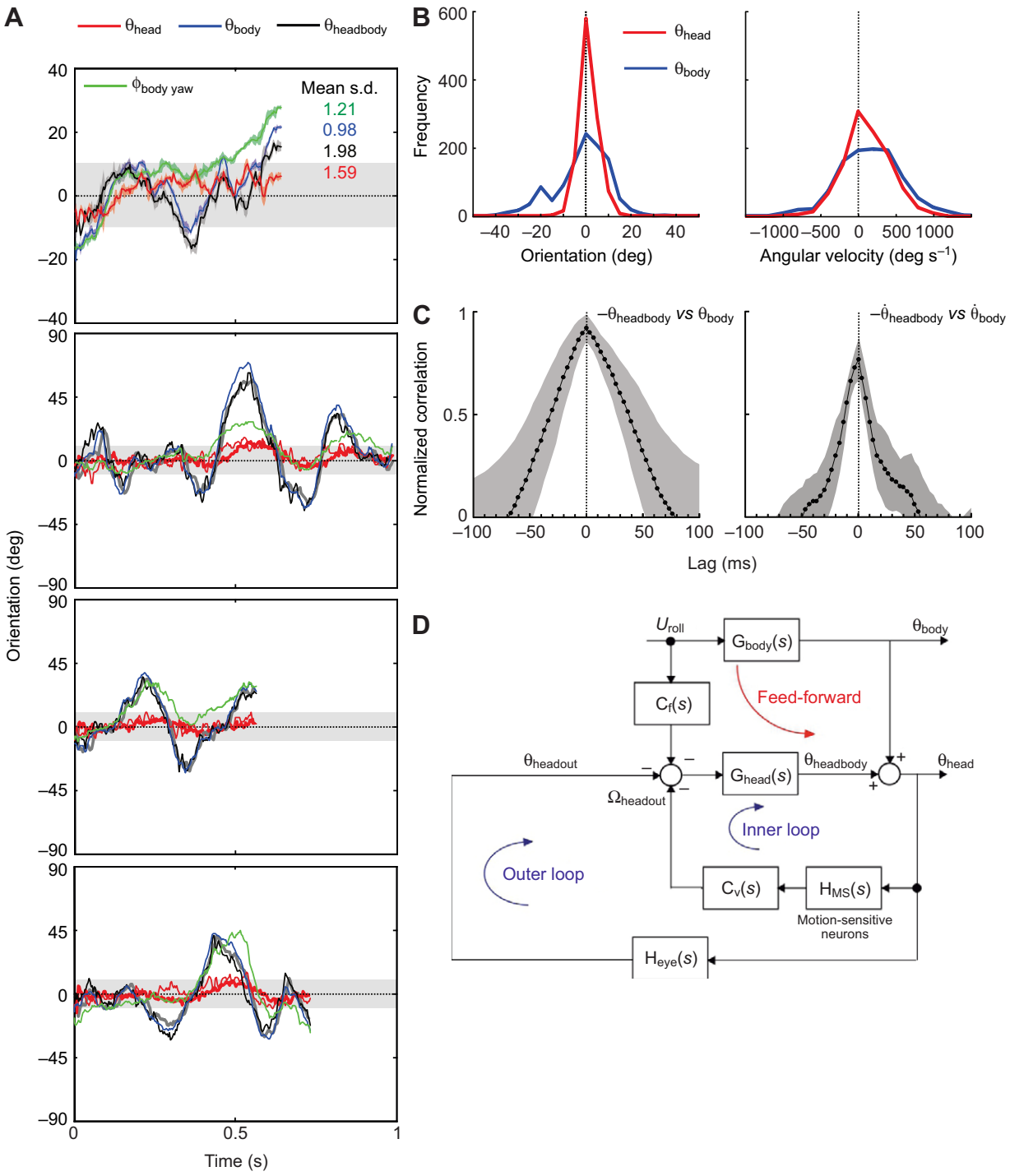


Fig. 7. Head roll control in free flight. (A) Time course of body orientation relative to vertical (blue), head orientation relative to horizontal (red), the inverse of head orientation relative to the body (black) and the yaw orientation of the body longitudinal axis (green) of patrolling *Polistes* males for four example sequences recorded at 300 frames $s^{-1}$. The sequence in the top panel has been digitized five times, with means (thick lines) and s.d. (shaded areas) shown in equivalent colours. Inset numbers are mean s.d. for the four variables. The horizontal grey areas in all panels mark ±10 deg. (B) Left: histograms of head orientation relative to horizontal (red) and body orientation relative to vertical (blue); right: histograms of angular velocity of head (red) and body (blue); data from 13 sequences, where wasp yaw orientation was within ±10 deg parallel to the optical axis of the camera; 3.75 s total flight time. (C) Mean cross-correlation functions (black dotted lines) with s.d. (grey shaded areas) for the same data set as used in (B). Left: head orientation relative to the body ($\theta_{headbody}$) against body orientation ($\theta_{body}$); right: head angular velocity relative to the body ($\theta_{headbody}/dt$) against body angular velocity ($\theta_{head}/dt$). (D) Expanded block diagram of the proposed head stabilization system in *Polistes* wasps including a feed-forward controller $C_f(s)$ that leads in principle to an exact compensation of head orientation ($\theta_{headbody}$) during spontaneous rotations of the body ($\theta_{body}$). The common drive signal $U_{roll}$ controls both head and body roll orientation, while the two nested visual feedback loops (see Fig. 6A) provide an absolute orientation reference and correct any remaining slip speed (for details see text). Without any recording of the signal $U_{roll}$, model responses $\theta_{head}(t)$ (thick grey lines) and $\theta_{headbody}(t)$ (thick red lines) plotted in A were computed by taking measured body orientation $\theta_{body}(t)$ (blue lines) as input signal for $C_f(s)$ and as input disturbance for the two nested visual feedback loops.

and

$$\hat{G}_{head}(s) = 1/0.65 . \quad (11)$$

In conclusion, the model results are in such close agreement with the free flight behaviour that we suggest a feed-forward control signal to be responsible for the fast compensatory head-roll movements in free flight.

## DISCUSSION

We have investigated compensatory head roll in *Polistes* wasps in tethered flight and found, at least in the frequency range we tested, no evidence for a haltere-like mechanosensory input that would help to compensate for imposed body roll movements. The extent of the visually driven compensation depends on the light intensity, possibly contrast and on the structure of the visual scene: compensation is best outdoors and becomes weaker under artificial light and visual conditions, such as in a laboratory scene, a 180 deg black and white pattern or a regular pattern of black and white stripes. Outdoors, wasps are able to maintain a constant, more or less horizontal head orientation after an imposed step rotation, indicating that an outdoor scene provides absolute orientation reference information, such as the overall light distribution or the sun. Wasps are unable to compensate for imposed body roll in uniform bright light and in total darkness. In free flight, wasps keep their head horizontal to within ±10 deg despite body roll amplitudes of ±40 deg and angular velocities up to at least 1000 deg $s^{-1}$.

Admittedly our samples are relatively small and the results of studying control systems in tethered flight need to be interpreted with caution: the tether interferes with the flexible properties of the thorax and in many other respects does not represent free flight conditions. However, within these limits, our results are consistent across animals and stimulus regimes and our free flight analysis suggests that rotation speed and amplitudes were comparable to those occurring most frequently in natural flight. Our data also demonstrate that there are significant differences in how control systems work even in tethered flight, depending on whether they are presented with artificial compared with naturalistic input.

There are a number of reasons why compensatory reflexes in response to imposed body rotations can be expected to perform more reliably under natural conditions. Both photoreceptors (Laughlin and Weckström, 1993; Tatler et al., 2000; Juusola and Hardie, 2001a; Juusola and Hardie, 2001b) and motion-sensitive interneurons (e.g. Egelhaaf et al., 2001; Lewen et al., 2001) become faster and more reliable as temperature and/or light levels increase. For instance, the response latency and the response reliability of the motion-sensitive H1 neuron in blowflies increases significantly with a 8°C increase in temperature (Egelhaaf et al., 2001), the response speed and temporal resolving power of fly photoreceptors more than double across the temperature range from 19 to 34°C (Tatler et al., 2000) and the information capacity of fly photoreceptors and ocellar interneurons increases with both light intensity and temperature (Juusola and Hardie, 2001a; Juusola and Hardie, 2001b; Simmons, 2011). However, there are many other significant differences between our artificial visual environments and the natural one, such as the distribution of light across the terrestrial and celestial hemispheres, including its spectral composition, its state of polarization and its spatial frequency spectrum. For all these reasons we probably obtained weaker responses under indoor illumination conditions and when wasps were surrounded by a structured environment composed of a regular black and white stripe pattern.

These differences are probably related to the different visual input channels that are known to be involved in the stabilization of the head around the roll axis in insects (for reviews, see Hengstenberg, 1993; Taylor and Krapp, 2007). Wasps, like flies and dragonflies, possess ocelli that function as fast horizon sensors (Stange, 1981; Berry et al., 2006; Berry et al., 2007), but are also involved together with the compound eyes in the dorsal light reflex (e.g. Hengstenberg, 1993; Schuppe and Hengstenberg, 1993; Parsons et al., 2010). Our successful modelling of step responses required in addition to a velocity servo that minimizes residual image motion across the eye, a position servo that adjusts the absolute orientation of the head. The input to this position servo could either be the overall light distribution such as in the tonic dorsal light response mediated by the compound eyes (cf. Hengstenberg, 1993) or the position of visual features across the visual field that would be most salient in the outdoor condition. It is not clear at this stage whether the ocelli in wasps could also provide positional information, as they do in dragonflies (Stange, 1981). In our model, we did not consider a phasic component of the dorsal light response, such as it is elicited by the ocelli in *Calliphora* (Hengstenberg, 1993; Schuppe and Hengstenberg, 1993). However, for the head roll stabilization, the fast high-pass filtering function of the ocelli could clearly complement the slower low-pass filter of the compound eyes.

Under all experimental conditions, we found the gain of the head roll compensation to be smaller than one, while in free flight, the wasps were perfectly able to keep their head horizontal at very similar thorax roll amplitudes and angular velocities. We see this as a reminder of two crucial problems with tethered flight experiments: (1) tethered flight interferes severely with the complicated mechanical properties of the thorax flight motor system, including the prosternal organs that may be involved in a mechanoreceptive feedback on head position relative to the thorax, and (2) it neglects the normal, active state of flight because it prevents feed-forward signals from playing their potentially crucial role in controlling head orientation during spontaneous flight manoeuvres.

In flies, the angular position of the head relative to the body is controlled in closed-loop by means of the prosternal organs (Preuss and Hengstenberg, 1992; Gilbert and Bauer, 1998; Paulk and Gilbert, 2006). For instance, it takes less than 300 ms for a flesh fly to compensate for an angular perturbation of 35 deg applied to the head (Gilbert and Bauer, 1998) and only 30 ms for a black soldier fly to pitch its head by 30 deg (Paulk and Gilbert, 2006). We are not aware that the mechanical and mechanosensory coupling between head and thorax has been investigated in *Polistes* wasps. There do not appear to be specific structures such as the prosternal organ, but extensive hair fields across the posterior cuticle of the head that may be in contact with the anterior parts of the thorax (J.Z., personal observation). We are thus not in the position to explain our observation that during the step response in the dark the head appears initially to be rigidly locked to the thorax and then overshoots in the direction of rotation. If head rotation would be solely governed by inertia in this situation the head would first stay behind and then be pulled in the direction of rotation by some spring or arresting properties of the neck connective. Schilstra and Hateren (Schilstra and Hateren, 1999; Hateren and Schilstra, 1999) assumed that in the fly *Calliphora* the thorax weighs about 100 mg and the head about 10 mg. That ratio appears to be only two in wasps, because in our model given in Fig. 7, we obtained a good fit of behavioural performance with body dynamics [$G_b(s)$] two times larger than those of the head. It is clearly of interest to determine body dynamics in hymenopteran insects in more detail in future studies.

Unlike blowflies, which execute fast body roll rotations of up to 2000 deg s$^{-1}$ (Schilstra and Hateren, 1999), with a maximum amplitude of ±90 deg (Hengstenberg, 1988), *Polistes* wasps – as our free flight analysis shows – are sluggish fliers, with long dangling legs extended during flight that lead to slower thorax roll dynamics and therefore requiring head roll compensation of much smaller and slower body rotations (see Fig. 7). Head stabilization outdoors and indoors does become more accurate with increasing frequency up to 2 Hz in *Polistes* wasps (see Bode diagrams in Fig. 3B) and in free flight, both wasps and honeybees (Boeddeker and Hemmi, 2010) are able to stabilize their head roll orientation to within ±10 deg of the horizontal despite body roll oscillations as large as ±45 deg. Boeddeker and Hemmi (Boeddeker and Hemmi, 2010) found this to be true in flying honeybees up to maximum roll velocities of 300 deg s$^{-1}$, which is slightly lower compared with the velocities experienced in natural flight by *Polistes* males (Fig. 7C). We did not detect a noticeable time lag between body roll movements and compensatory head movements in wasps, confirming what Boeddeker and Hemmi (Boeddeker and Hemmi, 2010) found in freely flying honeybees responding to a rotating pattern. Although such zero-delay responses could theoretically be due to non-linearities and temporal filter properties in the visual pathway, we propose here a vision-based feedback control scheme enhanced by a feed-forward control of the head orientation (see Fig. 7). When compensation is effective (see Figs 5, 6), the presence of overshoot in step responses can be explained in our model by a high gain of the visual controller $C_v(s)$.

We note that the time delay we measured in the chirp response analysis can result from a combination of a pure delay that shifts a signal by a fixed amount along the time axis, regardless of its frequency and of phase shifts caused by temporal filters in the signal processing pathways. However, as we did not notice any pure time delay in the step responses, the transfer functions of model responses to 45 deg step changes (Fig. 6) do not include any terms accounting for time delays.

The issue of zero-lag responses during spontaneous movements in free flight needs to be addressed in future experiments, possibly using suspended insects that can rotate freely, so that the time lag between compensatory head movements and rotating visual patterns can be accurately determined. This would also make it possible to identify the cut-off frequency of the visual feedback loops.

*Polistes* wasps, like all hymenopteran insects, do not possess modified wings such as the halteres of Diptera and Strepsiptera, and wing mechanoreceptors do not appear to provide a fast feed-forward signal of body rotations that could be used to adjust head orientation with a very small latency [about 3–5 ms in blowflies (Sandeman and Markl, 1980; Hengstenberg, 1993)]. Flying wasps never exhibited head compensation in the absence of image motion at imposed body roll frequencies ranging from 0.2 to 2 Hz and in response to step changes in body roll. As in honeybees (Boeddeker and Hemmi, 2010), gaze stabilization in *Polistes* wasps during enforced thorax roll oscillations thus clearly relies predominantly on visual feedback, involving motion-sensitive interneurons, which by necessity introduces much longer latencies than non-visual, open-loop haltere-derived oculomotor reflexes. In *Polistes* wasps, the largest time delay we found due to phase shift is about 80 ms, comparable to the 30 ms measured in blowflies (Hengstenberg, 1993). An alternative possibility is that our maximal turning velocity of 245 deg s$^{-1}$ was too slow to stimulate potential Coriolis force sensors on the wings. However, halteres in both Diptera and Strepsiptera do respond to rotational velocities as low as 100 deg s$^{-1}$ (Hengstenberg, 1993; Pix et al., 1993), so that this is an unlikely reason for why we did not find mechanosensory input to the head roll control system in *Polistes*.

It remains to be shown how head roll orientation is controlled in some of the fast flying and hovering Hymenoptera, such as *Bembix* wasps and *Amegilla* bees. *Bembix* wasps, for instance, execute fast saccadic sideways translations by extreme body roll movements of up to 180 deg amplitude at 2−4000 deg s$^{-1}$ during which the head remains nearly perfectly horizontal (Zeil et al., 2008). A possibility is that the motion-sensitive neurons in these hovering Hymenoptera are tuned to higher image velocities, as has been shown to be the case in hoverflies and bumblebees (O'Carroll et al., 1996). However, our analysis here suggests that during spontaneous body roll movements, head orientation may be largely controlled by a feed-forward signal, where a copy of the command signals to the wing motoneurons is sent with an opposite sign to the head position servo system (for review, see Webb, 2004). In our model, contrary to what has been considered by Varju (Varju, 1990) and Collett (Collett, 1980), the efference copy of the control input signal $U_{roll}$ does not interfere with the inner and the outer visual feedback loops, in the sense that it does not cancel the control input signals $\theta_{headout}$ and $\Omega_{headout}$ to make the head rotate. Our model is also different from the one proposed by Chan et al. (Chan et al., 1998), because it does not rely on inhibition of, or a bias introduced in, a sensor (the halteres in this case). Unlike that suggested by the reafference (von Holst and Mittelstaedt, 1950), or corollary discharge principle (Sperry, 1950), the output of our forward model [$C_f(s)$] does not serve as input to a sensory processing unit (for review, see Webb, 2004), but controls head orientation in such a way that spontaneous roll body movements do not induce image motion, because the head remains horizontally aligned. In our model, the control signal $U_{roll}$ can be considered as an input reference for controlling the orientation of the body around the roll axis. The wasp could benefit from a passive roll stability of its body (see supplementary material Movies 1−3 of free flight) with a centre of mass placed below the centre of thrust. The feed-forward control proposed here relies only on an accurate internal model of the body's dynamics [$C_f(s)$]. In the model shown in Fig. 7E, the control input signal $U_{roll}$ is copied and sent to the feed-forward controller $C_f(s)$. The latter improves dramatically the performance of the gaze stabilization system during spontaneous rotation of the body because it compensates for the negative phase shift inherent in the two visual feedback loops. Similar feed-forward control has been suggested to explain the high accuracy of vertebrate gaze stabilization during self-generated body movements (Combes et al., 2008) and has been successfully implemented in the gaze stabilization system of a sighted aerial robot (Kerhuel et al., 2010). We found no delay between head and thorax movements in freely flying *Polistes* wasps and take this as a strong indication that head roll stabilization does involve feed-forward control signals that are inherently difficult to detect and to study in tethered flight. One testable prediction would be that spontaneous changes in wing movements during tethered flight should trigger brief head movements in the opposite direction to the intended body roll rotation.

## ACKNOWLEDGEMENTS

We thank Waltraud Pix for her help with movie film analysis, Mark Snowball for advice and Franck Ruffier for fruitful discussions. Marc Boyron assisted in designing and producing the control electronics and the LabVIEW programs. We also thank Julien Diperi for his help with the mechanical construction of the set-up.

## AUTHOR CONTRIBUTIONS

Both authors made equal contributions to the conception, design and execution of experiments, to the interpretation of the findings, and to the drafting and revisions of the article.

## FUNDING

This work received support from the Australian Research Council Centre of Excellence program (CE0561903 to J.Z.) and from the Centre for Visual Sciences at the Australian National University (to S.V.). In addition, S.V. acknowledges support from the Centre National de la Recherche Scientifique (CNRS), Aix-Marseille University, the Agence Nationale de la Recherche (ANR) [with the EVA project (Autonomous Flying Entomopter) and the IRIS project (Intelligent Retina for Innovative Sensing) ANR-12-INSE-0009].

## REFERENCES

**Berry, R., Stange, G., Olberg, R. and van Kleef, J.** (2006). The mapping of visual space by identified large second-order neurons in the dragonfly median ocellus. *J. Comp. Physiol. A* **192**, 1105-1123.

**Berry, R., van Kleef, J. and Stange, G.** (2007). The mapping of visual space by dragonfly lateral ocelli. *J. Comp. Physiol. A* **193**, 495-513.

**Boeddeker, N. and Hemmi, J. M.** (2010). Visual gaze control during peering flight manoeuvres in honeybees. *Proc. Biol. Sci.* **277**, 1209-1217.

**Boeddeker, N., Dittmar, L., Stürzl, W. and Egelhaaf, M.** (2010). The fine structure of honeybee head and body yaw movements in a homing task. *Proc. R. Soc. B* **277**, 1899-1906.

**Chan, W. P., Prete, F. and Dickinson, M.** (1998). Visual input to the efferent control system of a fly's 'gyroscope'. *Science* **280**, 289-292.

**Collett, T. S.** (1980). Angular tracking and the optomotor response. An analysis of visual reflex interaction in a hoverfly. *J. Comp. Physiol.* **140**, 145-158.

**Combes, D., Le Ray, D., Lambert, F. M., Simmers, J. and Straka, H.** (2008). An intrinsic feed-forward mechanism for vertebrate gaze stabilization. *Curr. Biol.* **18**, R241-R243.

**Dickinson, M. H.** (1999). Haltere-mediated equilibrium reflexes of the fruit fly, *Drosophila melanogaster*. *Philos. Trans. R. Soc. Lond. B* **354**, 903-916.

**Egelhaaf, M., Grewe, J., Kern, R. and Warzecha, A. K.** (2001). Outdoor performance of a motion-sensitive neuron in the blowfly. *Vision Res.* **41**, 3627-3637.

**Fox, J. L. and Daniel, T. L.** (2008). A neural basis for gyroscopic force measurement in the halteres of Holorusia. *J. Comp. Physiol. A* **194**, 887-897.

**Frye, M. A.** (2009). Neurobiology: fly gyro-vision. *Curr. Biol.* **19**, R1119-R1121.

**Gilbert, C. and Bauer, E.** (1998). Resistance reflex that maintains upright head posture in the flesh fly *Neobellieria bullata* (Sarcophagidae). *J. Exp. Biol.* **201**, 2735-2744.

**Hengstenberg, R.** (1988). Mechanosensory control of compensatory head roll during flight in the blowfly *Calliphora erythrocephala* Meig. *J. Comp. Physiol. A* **163**, 151-165.

**Hengstenberg, R.** (1993). Multisensory control in insect oculomotor systems. In *Visual Motion and its Role in the Stabilization of Gaze* (ed. F. A. Miles and J. Wallmann), pp. 285-298. Amsterdam: Elsevier.

**Huston, S. J. and Krapp, H. G.** (2009). Non-linear integration of visual and haltere inputs in fly neck motor neurons. *J. Neurosci.* **29**, 13097-13105.

**Juusola, M. and Hardie, R. C.** (2001a). Light adaptation in *Drosophila* photoreceptors: I. Response dynamics and signaling efficiency at 25°C. *J. Gen. Physiol.* **117**, 3-25.

**Juusola, M. and Hardie, R. C.** (2001b). Light adaptation in *Drosophila* photoreceptors: II. Rising temperature increases the bandwidth of reliable signaling. *J. Gen. Physiol.* **117**, 27-42.

**Kerhuel, L., Viollet, S. and Franceschini, N.** (2010). Steering by gazing: an efficient biomimetic control strategy for visually-guided micro-air vehicles. *IEEE Trans. Robot.* **26**, 307-319.

**Krapp, H. G., Hengstenberg, B. and Hengstenberg, R.** (1998). Dendritic structure and receptive-field organization of optic flow processing interneurons in the fly. *J. Neurophysiol.* **79**, 1902-1917.

**Laughlin, S. B. and Weckström, M.** (1993). Fast and slow photoreceptors – a comparative study of the functional diversity of coding and conductances in the diptera. *J. Comp. Physiol. A* **172**, 593-609.

**Lewen, G. D., Bialek, W. and de Ruyter van Steveninck, R. R.** (2001). Neural coding of naturalistic motion stimuli. *Network* **12**, 317-329.

**Ljung, L.** (1996). *System Identification: The Control Handbook* (ed. W. S. Levine), pp. 1033-1054. Boca Raton, FL: CRC Press.

**Ljung, L.** (1999). *System Identification: Theory For The User*. Upper Saddle River, NJ: PTR Prentice Hall.

**Nalbach, G.** (1993). The halteres of the blowfly *Calliphora*. I. Kinematics and dynamics. *J. Comp. Physiol. A* **173**, 293-300.

**Nalbach, G.** (1994). Extremely non-orthogonal axes in a sense organ for rotation: behavioural analysis of the dipteran haltere system. *Neuroscience* **61**, 149-163.

**Nalbach, G. and Hengstenberg, R.** (1994). The halteres of the blowfly *Calliphora*. II. 3-Dimensional organization of compensatory reactions to real and simulated rotations. *J. Comp. Physiol. A* **175**, 695-708.

**O'Carroll, D. C., Bidwell, N. J., Laughlin, S. B. and Warrant, E. J.** (1996). Insect motion detectors matched to visual ecology. *Nature* **382**, 63-66.

**Parsons, M. M., Krapp, H. G. and Laughlin, S. B.** (2010). Sensor fusion in identified visual interneurons. *Curr. Biol.* **20**, 624-628.

**Paulk, A. and Gilbert, C.** (2006). Proprioceptive encoding of head position in the black soldier fly, *Hermetia illucens* (L.) (Stratiomyidae). *J. Exp. Biol.* **209**, 3913-3924.

**Pix, W., Nalbach, G. and Zeil, J.** (1993). Strepsipteran forewings are haltere-like organs of equilibrium. *Naturwissenschaften* **80**, 371-374.

**Preuss, T. and Hengstenberg, R.** (1992). Structure and kinematics of the prosternal organs and their influence on head position in the blowfly *Calliphora erythrocephala* Meig. *J. Comp. Physiol. A* **171**, 483-493.

**Sandeman, D. C. and Markl, H.** (1980). Head movements in flies (*Calliphora*) produced by deflection of the halteres. *J. Exp. Biol.* **85**, 43-60.

**Sane, S. P., Dieudonné, A., Willis, M. A. and Daniel, T. L.** (2007). Antennal mechanosensors mediate flight control in moths. *Science* **315**, 863-866.

**Schilstra, C. and van Hateren, J. H.** (1999). Blowfly flight and optic flow. I. Thorax kinematics and flight dynamics. *J. Exp. Biol.* **202**, 1481-1490.

**Schuppe, H. and Hengstenberg, R.** (1993). Optical properties of the ocelli of *Calliphora erythrocephala* and their role in the dorsal light response. *J. Comp. Physiol. A* **173**, 143-149.

**Schwyn, D. A., Heras, F. J. H., Bolliger, G., Parsons, M. M., Krapp, H. G. and Tanaka, R. J.** (2011). Interplay between feedback and feedforward control in fly gaze stabilization. In *Proceedings of the IFAC World Congress*, *Milano*, pp. 9674-9679.

**Sherman, A. and Dickinson, M. H.** (2003). A comparison of visual and haltere-mediated equilibrium reflexes in the fruit fly *Drosophila melanogaster*. *J. Exp. Biol.* **206**, 295-302.

**Simmons, P. J.** (2011). The effects of temperature on signalling in ocellar neurons of the desert locust, *Schistocerca gregaria*. *J. Comp. Physiol. A* **197**, 1083-1096.

**Sperry, R. W.** (1950). Neural basis of the spontaneous optokinetic response produced by visual inversion. *J. Comp. Physiol. Psychol.* **43**, 482-489.

**Stange, G.** (1981). The ocellar component of flight equilibrium control in dragonflies. *J. Comp. Physiol.* **141**, 335-347.

**Tatler, B., O'Carroll, D. C. and Laughlin, S. B.** (2000). Temperature and the temporal resolving power of fly photoreceptors. *J. Comp. Physiol. A* **186**, 399-407.

**Taylor, G. K. and Krapp, H. G.** (2007). Sensory systems and flight stability: what do insects measure and why? *Adv. In Insect Phys.* **34**, 231-316.

**Varjú, D.** (1990). A note on the reafference principle. *Biol. Cybern.* **63**, 315-323.

**van Hateren, J. H. and Schilstra, C.** (1999). Blowfly flight and optic flow. II. Head movements during flight. *J. Exp. Biol.* **202**, 1491-1500.

**von Holst, E. and Mittelstaedt, H.** (1950). Das Reafferenzprinzip. *Naturwissenschaften* **37**, 464-476.

**Webb, B.** (2004). Neural mechanisms for prediction: do insects have forward models? *Trends Neurosci.* **27**, 278-282.

**Xia, X. G.** (1997). System identification using chirp signals and time-variant filters in the joint time-frequency domain. *IEEE Trans. Signal Process.* **45**, 2072-2084.

**Zeil, J., Boeddeker, N. and Hemmi, J. M.** (2008). Vision and the organization of behaviour. *Curr. Biol.* **18**, R320-R323.